Thermomechanical processing of a near-β titanium alloy and effects on microstructure and tensile properties

X. Jiang, C.-J. Zhang*, Z.-D. Lv, H. Feng, S.-Z. Zhang, C. Wang

College of Materials Science and Engineering, Taiyuan University of Technology, Taiyuan 030024, P. R. China

Abstract

This paper reports the response of microstructure and mechanical properties of a near-β Ti-4Al-1Sn-2Zr-5Mo-8V-2.5Cr (wt.%) alloy after thermomechanical processing. Microstructure observation shows that the precipitation of the primary α phase depends on solution temperature. The highest volume fraction and the smallest size of the secondary α phase precipitated after solution treatment near the phase transition point plus aged treatment at 480 °C. Schematic illustration of the microstructure evolution after different heat treatments was described. Compared with the alloy after solution treatment at β phase region, the alloy has higher ultimate tensile strength after solution treatment at α/β phase region owing to the alloy precipitates primary α phase. It was found that the alloy after solution treatment at 720 °C plus aging treatment at 440 °C has a better ultimate tensile strength of about 1611 MPa, the elongation of about 2.53 %. The main reason is that the precipitation of the secondary α phase contributed to tensile properties substantially.

K e y w o r d s: near-β titanium alloy, thermomechanical processing, microstructure, tensile properties

1. Introduction

Near β titanium alloy as aerospace structural material maintains a characteristic niche where high specific strength, corrosion resistance, and good formability are comparable with those of α and $\alpha+ \beta$ titanium alloys [1–4]. The preparation of superior near β high strength titanium alloy has become a significant study in the field of titanium alloy for the performance requirements of next-generation aerospace titanium alloy. As-cast β titanium alloys are usually accompanied by coarse β grain size, while the β grain size is an important factor affecting the mechanical properties of the alloy, especially the elongation [5–7]. In general, hot deformation is the most common method to improve the size of titanium alloy grains [8–10]. For near β titanium alloy, to satisfy the application requirements, only hot deformation is not enough. Multiple heat treatments are the necessary path to obtain ideal microstructure and mechanical properties. Previous studies demonstrated that the precipitation of primary α phase after solution treat-
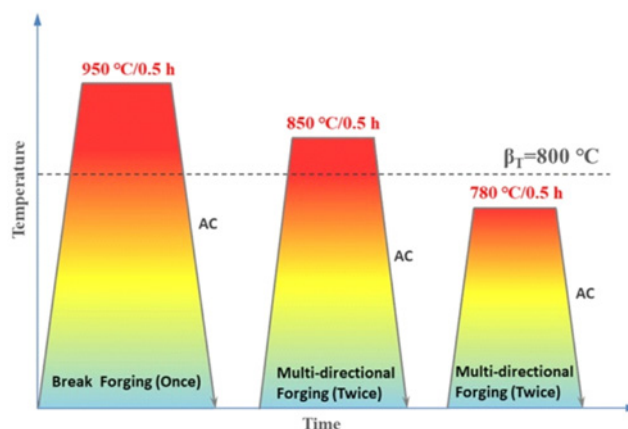

Fig. 1. Schematic illustration of the multidirectional forging process.

ment at α/β phase region has a pronounced effect on the refinement of β grain size [11, 12]. Du et al. [13] reported that the β grain size of Ti-3.5Al-5Mo--6V-3Cr-2Sn-0.5Fe (wt.%) alloy is 2 μm if the alloy is

*Corresponding author: tel./fax: +86-351-6010022, e-mail address: zhangchangjiang@tyut.edu.cn

T a b l e 1. The chemical composition of Ti-4Al-1Sn-2Zr-5Mo-8V-2.5Cr alloy (wt.%)

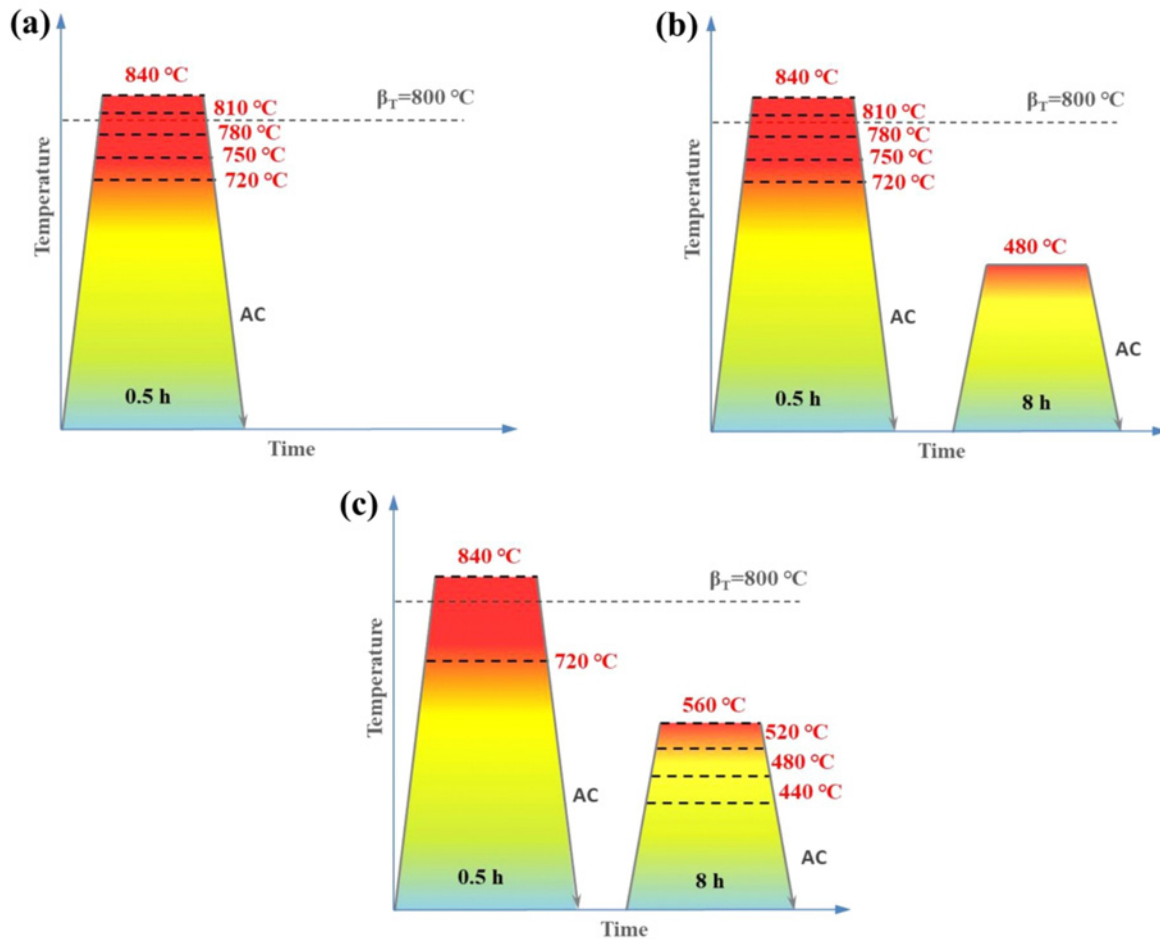| Elements	Al	Sn	Zr	Mo	V	Cr	Ti
Nominal content	4.00	1.00	2.00	5.00	8.00	2.50	bal.
Actual content	4.30	1.03	2.07	4.99	8.00	2.50	bal.

Fig. 2. Schematic diagrams of heat treatment: (a) solution treatment at different temperatures, (b) aging treatment at 480 ℃ after solution treatment at different temperatures, (c) aging treatment at different temperatures after solution treatment at 840 and 720 ℃.

solutionized in the α/β phase region, which leads to higher alloy strength. Fan et al. [14] observed that the volume fraction of spherical primary α phases precipitated from Ti-7333 alloy decreases with solution temperature increasing. The acicular secondary α phase, obtained by the transformation of metastable β phases during aging treatment, controls the strength level of the alloy due to the dispersed particles strengthening mechanism [15, 16]. Banerjee et al. [17] noted that the hardness of the α phase is higher than that of the β phase owing to its high solid solubility to Al and Zr elements. Therefore, compared with the β phase, the acicular secondary α phase is difficult to be sheared by dislocation and accounts for the exceptional alloy strength. Mantri et al. [18] reported that the ultimate

tensile strength of the commercially available β-21S alloy is increased to 1810 MPa by tailoring the scale of the secondary α phase. Zhu et al. [19] suggested that the moderate length of α lamellar spacing can also effectively increase the strength of the alloy. However, the secondary α phase leads to a sharp decrease in the elongation of the alloy, which limits the application of the alloy [20, 21].

At present, about a near-β Ti-4Al-1Sn-2Zr-5Mo-8V-2.5Cr alloy, previous studies focused on the hot compression behavior and as-forged microstructure evolution of the alloy [22, 23]. However, the sensitivity of α phase precipitated to heat treatment parameters is not clear, and the optimal tensile strength and elongation combination degree is still not obtained.
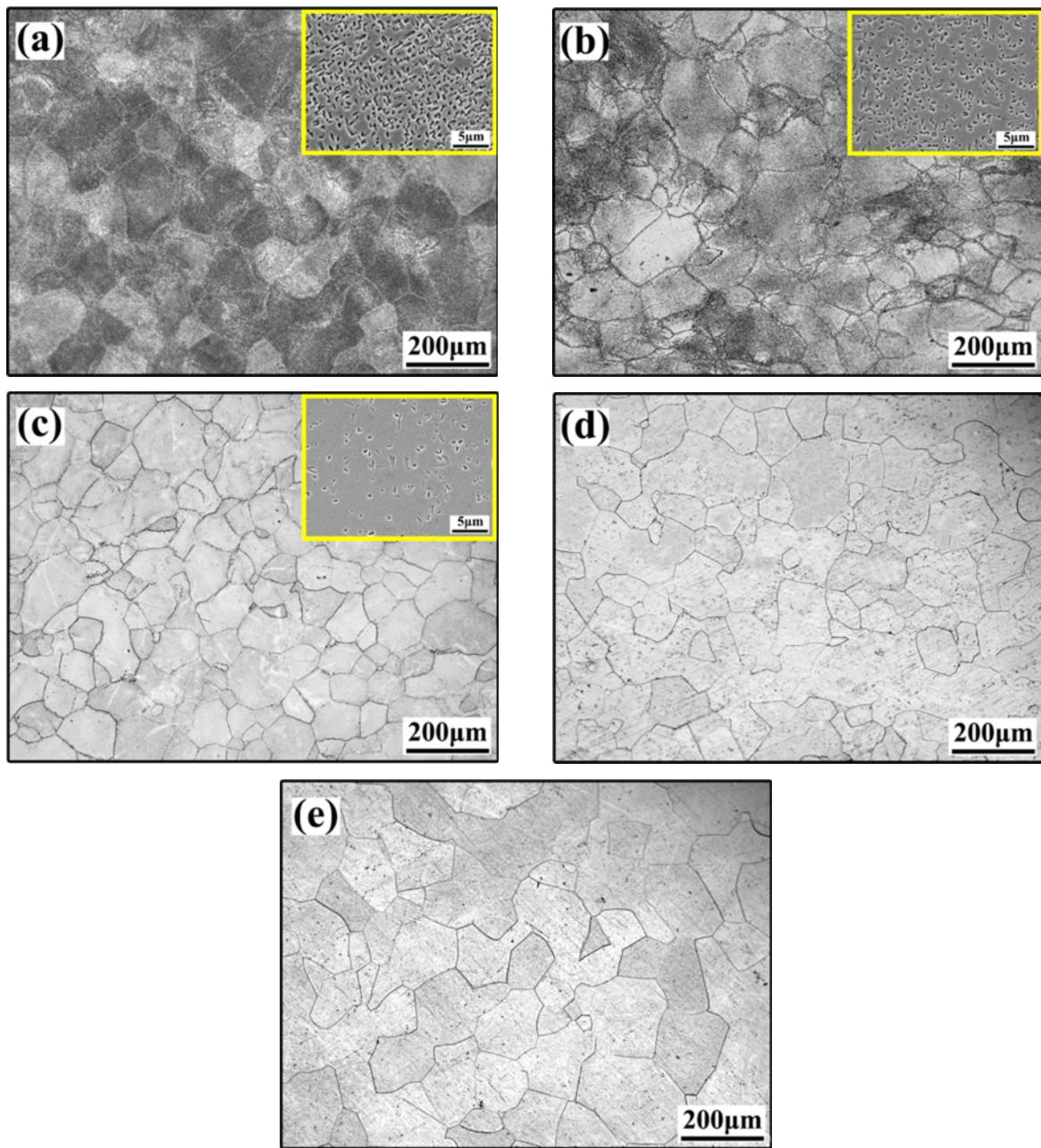
Fig. 3. Microstructures of the forged alloy after solution treatment at α/β phase region: (a) 720 °C, (b) 750 °C, (c) 780 °C. The inset of (a), (b), and (c) shows SEM view local characteristics of these OM images, clearly showing the precipitation of primary α phase. After solution treatment at β phase region: (d) 810 °C, (e) 840 °C.

Therefore, in the present investigation, the precipitation behavior of α phase of the as-forged alloy after solution treatment at α/β and β phase region and aging at different temperatures was characterized and related these to fundamental mechanical properties.

2. Material and experimental procedures

The near-β Ti-4Al-1Sn-2Zr-5Mo-8V-2.5Cr alloy is discussed in this paper. Alloy raw material (purity Ti

and Zr sponge, Al and Cr ingot, and Al-Mo and Al-V master alloy) was melted by the twice vacuum Induction Skull Melter (ISM) melting technique; the detailed chemical composition is shown in Table 1. The β transformation temperature was estimated forging were carried out for a more uniform ingot structure. The processing route is illustrated in Fig. 1, and the deformation rate was $2\,\mathrm{mm\,s^{-1}}$. The microstructure of as-forged alloy was reported elsewhere [23]. All heat-treated samples were cut from as-forged alloy used wire electro-discharge machining (WEDM) technol-

ogy. Solution treatment at α/β phase region (720, 750, and 780 °C) and β phase region (810 and 840 °C) for 0.5 h followed by air cooling were conducted for all samples. Subsequently, the samples were subjected to aging at temperatures ranging from 440 to 560 °C for 8 h and followed by air cooling. The schematic diagram of heat treatment is shown in Fig. 2.

Samples for metallographic observation were mechanically ground on 80–2000 grit sandpaper, electrochemically polished, and etched in a standard Kroll's reagent (3 % HF, 5 % HNO_3, and 92 % H_2O). Analysis of microstructural characterization was carried out on DM2700MRL optical microscope (OM) and Quanta 200FEG scanning electron microscope (SEM). APD--10 X-ray diffraction (XRD) was performed for phase identification of the composite. The ambient temperature tensile properties were tested on INSTRON--5500R electronic universal material testing machine with a constant speed of 0.5 mm min^{-1}. The cross--section of the gauge length part of the tensile specimen at room temperature is 4×2 mm^2, and the longitudinal section is 18×2 mm^2. To obtain the strain during axial tension accurately, a 12 mm contact extensometer is clamped on the gauge part of the tensile specimen. Three sets of testing data with the same condition are required to obtain a more accurate result.

3. Results and discussion

3.1. Primary α phase and β grain

The microstructures of titanium alloy Ti-4Al-1Sn--2Zr-5Mo-8V-2.5Cr at different solution conditions are examined in Fig. 3. The SEM micrographs inset on the top right corner of Figs. 3a–c shows that the equiaxed primary α phase precipitates in β grains after solution treatment at α/β phase region (720, 750, and 780 °C). The stored energy during hot deformation is beneficial to forming equiaxed α phase morphology [24]. With the increase of solution temperature, the volume fraction of the primary α phase decreases from 27 to 2 %. This phenomenon can be explained by the primary α phase dissolution rate, which increases with the solution temperature [25]. Particularly, as a large amount of the primary α phase is dissolved into the matrix, the volume fraction of α phase (2 vol.%) after solution temperature at 780 °C sharply decreases, as shown in Fig. 3c. Meanwhile, owing to the higher Mo equivalent of the alloy (11.1) and the limiting effect of the β-stable element on the α phase, there is no coarsening of the primary α phase [23, 26, 27]. It can be seen from Figs. 3a–c that the average grain size of recrystallized β grain increases from 104 to 138 µm with increasing solution temperature from 720 to 780 °C. Recrystallization of β grain is restricted by the exis-
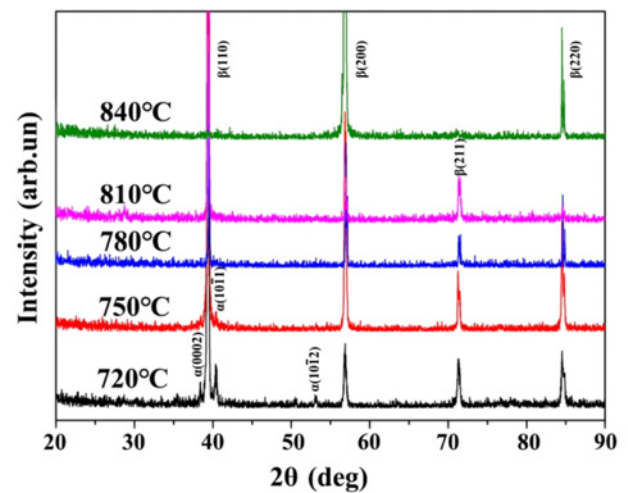

Fig. 4. X-ray diffraction spectra of Ti-4Al-1Sn--8V-2.5Cr alloy after solution treatment at different temperatures.

tence of primary α phase on β grain boundary [11, 28, 29], thereby the size of β phase is increasing with the volume fraction of α phase decreasing. After solution treatment at β phase region (810 and 840 °C), according to Figs. 3d,e, the degree of recrystallization increases and the β grains grow up.

Figure 4 shows the XRD results of the corresponding temperature. The diffraction peak of the α phase is weaker than that of the β phase owing to the rarity of the α phase, and it disappears entirely at the β phase region. The XRD analysis results further confirmed the above observation of microstructure.

3.2. Secondary α phase

3.2.1. Solution treatment at different temperatures plus aging treatment

Figure 5 exhibits microstructures of the alloy after solution treatment at different temperatures plus aging treatment at 480 °C. As shown in Figs. 5a–c, the acicular secondary α phase precipitates are uniformly distributed within the matrix. The variation trend of secondary α phase below (Figs. 5a–c) and above (Figs. 5d,e) the phase transition point is opposite. The acicular secondary α phase with the largest volume fraction and the smallest size precipitates in alloy after solution treatment near the phase transition point plus aging treatment, as seen in Fig. 5c. Generally, the precipitation of the secondary α phase is related to the stability of the β phase [30]. The less (Fig. 5c) precipitation of the primary α phase from β matrix after solution treatment near the phase transition point leads to decrease of the stability of the β matrix, and the driving force for the nucleation of
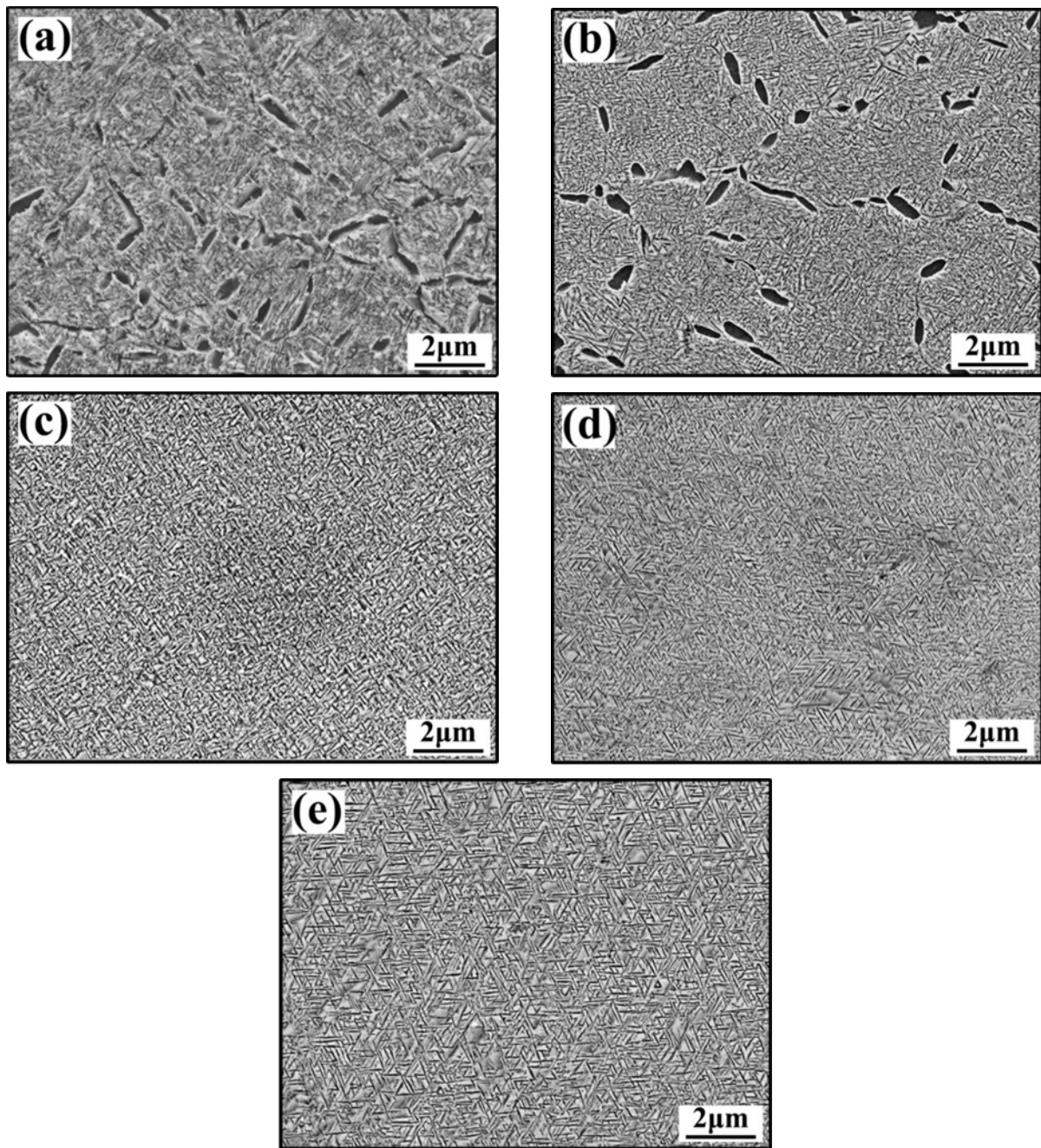
Fig. 5. Microstructures of alloy after solution treatment at (a) 720 ℃, (b) 750 ℃, (c) 780 ℃, (d) 810 ℃, and (e) 840 ℃ for 0.5 h plus aging treatment at 480 ℃ for 8 h.

the secondary α phase was strengthened in the subsequent aging process, which results in more precipitation of secondary α phase [31, 32]. But it also limits the growth of the secondary α phase to some extent. Owing to lower β matrix stability with more α stable elements dissolved in β matrix after solution treatment in the β phase region, the secondary α phase precipitates at β phase region with a larger size, as shown in Figs. 5d,e. Microstructure evolution of the fact that the secondary α phase precipitated in the β phase region is coarser than that in the α/β region

was also reported in previous literature [33].

3.2.2. $\alpha + \beta$ solution treatment plus aging treatment at different temperatures

Figure 6 shows micrographs of samples solution treated at 720 ℃ (α/β phase region) plus aged at the temperature range from 440 to 560 ℃. As shown in Figs. 6a–d, a small amount of equiaxed primary α phase was generated and the fine-scale secondary α phase with acicular shape was distributed on the β
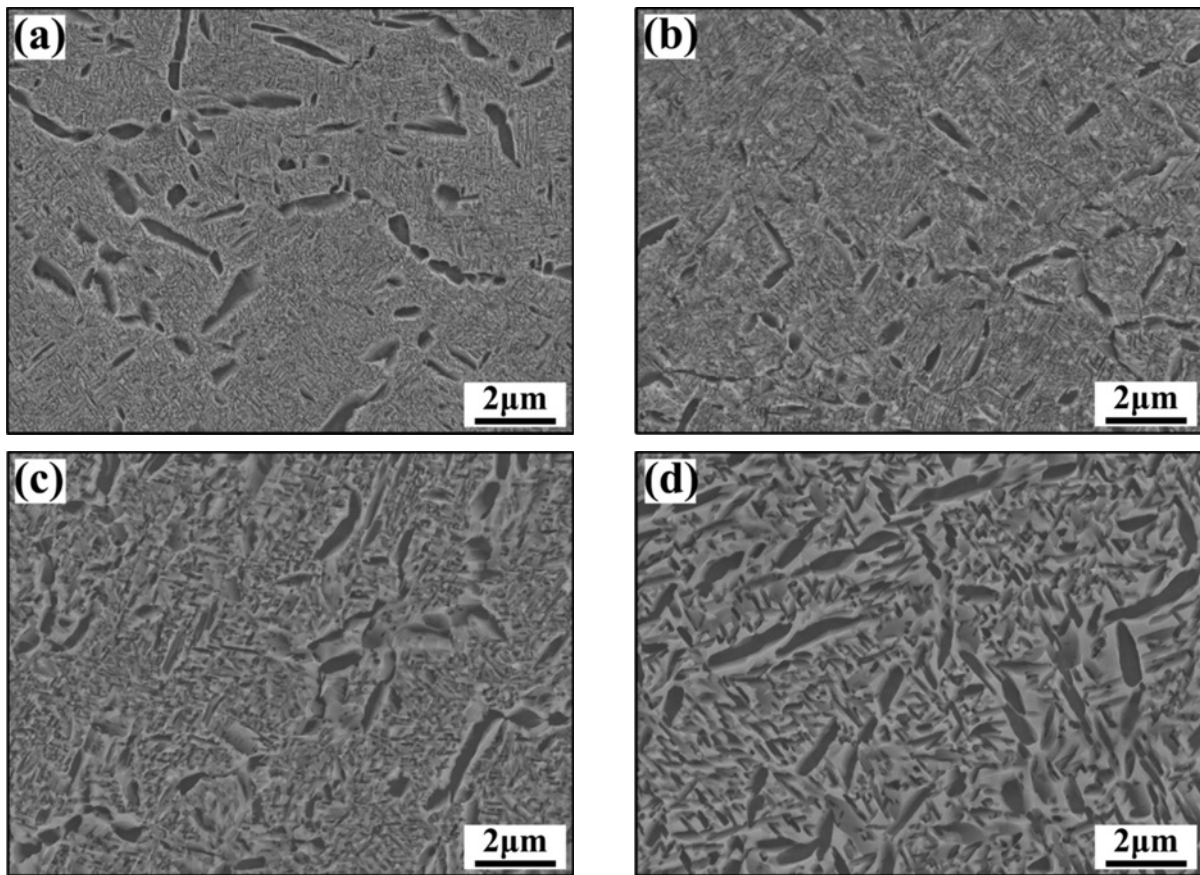
Fig. 6. Microstructures of the alloys after solution treatment at 720 ℃ plus aging treatment at: (a) 440 ℃, (b) 480 ℃, (c) 520 ℃, and (d) 560 ℃.

matrix. Comparing the influence of solution temperature (Fig. 5), there was no noticeable change in the volume fraction and size of the primary α phase with aging temperature increasing (Fig. 6). Conversely, the secondary α phase is unusually sensitive to aging temperature. As shown in Figs. 6a–d, with the increase of aging temperature, the volume fraction of the secondary α phase decreases while the size increases. Meanwhile, it is seen in Fig. 6d that the acicular secondary α phase transformed into rod-like structures. Some studies suggest that a lower aging temperature can provide a higher nucleation driving force for the secondary α phase but a lower growth driving force [12, 34]. For the near-β titanium alloy, the driving force of phase transformation originates from the difference of Gibbs free energy of α phase and β phase [35–37]. During aging treatment, the β phase with the higher Gibbs free energy will transform to the α phase with the lower Gibbs free energy to stabilize the whole system. Therefore, the difference of Gibbs free energy will decrease with the increase of aging temperature, resulting in the decrease of nucleation driving force of α phase and the precipitation of less secondary α phase. Other scholars found that the diffusion rate of elements also affects the growth of the α phase [38],

which means that the secondary α phase is easier to grow at a higher aging temperature.

3.2.3. β solution treatment plus aging treatment at different temperatures

Microstructures after solution treatment at 840 ℃ (β phase region) for 0.5 h plus aging treatment at different temperatures (from 440 to 560 ℃) for 8 h are shown in Fig. 7. The evolution trend of the secondary α phase after solution treatment at β phase region is similar with α/β phase region, as shown in Figs. 7a–d. After aging at 440 ℃, as shown in Fig. 7a, the secondary α phase is so fine that the β matrix and α phase are indistinguishable. The secondary α phase gradually can be observed with the increase of the aging temperature from 480 ℃ (Fig. 7b) to 520 ℃ (Fig. 7c). As shown in Fig. 7d, the size of the secondary α phase reaches the maximum (average width: 146 nm) after aging at 560 ℃. Meanwhile, compared with Fig. 6, it is found that the complete disappearance of the primary α phase (Fig. 7) and the volume fraction and size of the secondary α phase increases after solution treatment at 840 ℃ plus aging (Fig. 7). The main reason is that the least stable β matrix
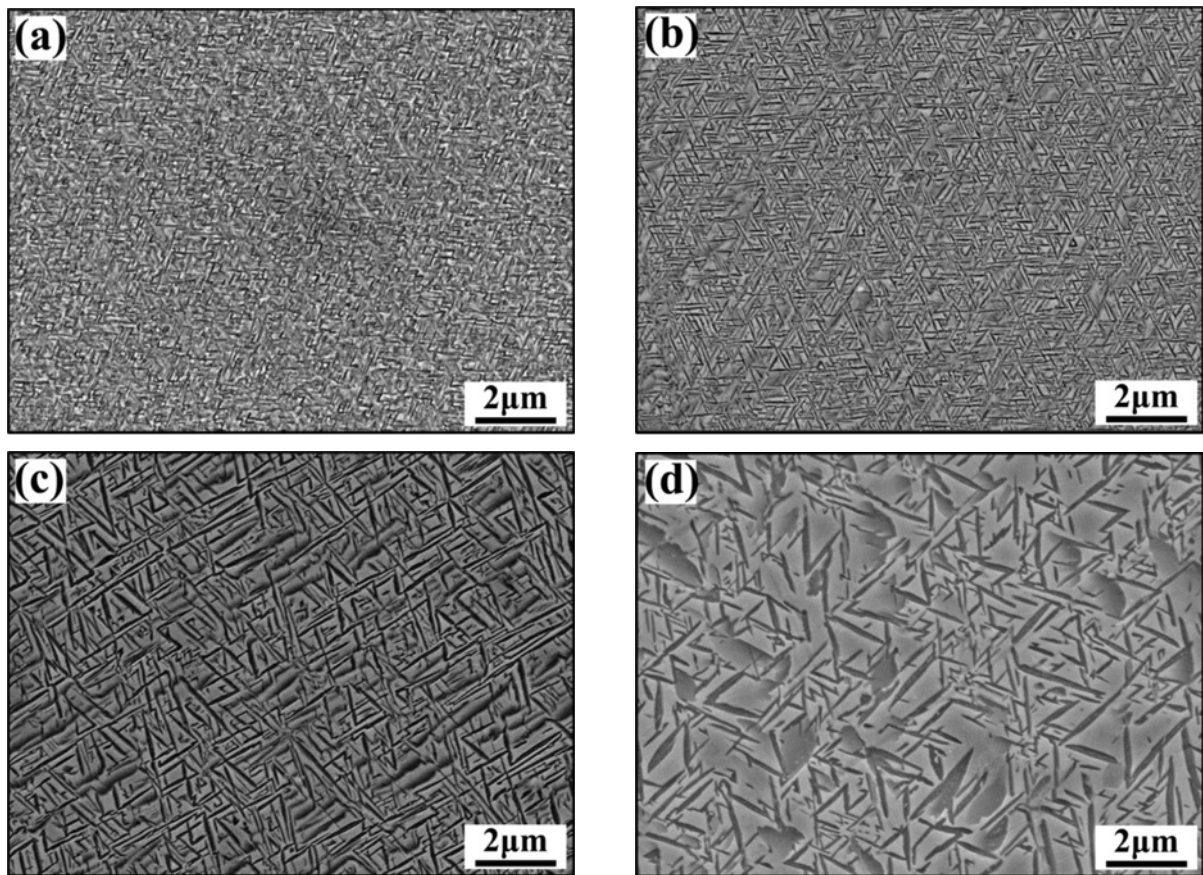
Fig. 7. Microstructures of the alloys after solution treatment at 840 °C plus aging treatment at: (a) 440 °C, (b) 480 °C, (c) 520 °C, and (d) 560 °C.

with no primary α phase precipitation strengthens the precipitation driving force of the secondary α phase during the aging treatment. Noticeably, the so-called un-aged or precipitate-free zone formed after aging treatment at 560 °C, as shown in Fig. 7d. This may be caused by insufficient driving force for nucleation. Lütjering et al. [39] suggested that the soft precipitate-free zone affected the elongation of the alloy.

The concise schematic illustration in Fig. 8 shows the microstructure evolution of a near-β Ti-4Al-1Sn-2Zr-5Mo-8V-2.5Cr alloy after different heat treatments. It can be seen that the β grain and primary α phase are mainly tailored by the solution temperature. Meanwhile, the stability of the β phase controlled by solution temperature affects the secondary α phase precipitation during subsequent aging. The volume fraction of the secondary α phase is the largest, and the size is the smallest after solution treatment near the phase transition point plus aging. The effect of aging temperature on the secondary α phase is the most important. With the increase of aging temperature, the nucleation driving force decreases, but the increase of growth of driving force results in the decrease of volume fraction and the increase of the size of the secondary α phase.

3.3. Tensile properties

Figure 9a gives the tensile properties of the alloy after solution treatment at different temperatures. It can be seen that the changing trend of strength and elongation after solution treatment at α/β phase region (from 720 to 780 °C) is opposite: the strength decreases from 967 to 793 MPa with the increase of temperature and the elongation increases from 3.41 to 5.72 %. This phenomenon is because the primary α phase in this state can significantly improve the strength of the alloy [31, 35]. As shown in Fig. 3, the volume fraction of the primary α phase decreases with the increase of solution temperature, which reduces its contribution to the strength of the alloy. While the trend at β phase region (810 and 840 °C) is identical, both strength and elongation increase (UTS: 737 and 809 MPa, EL: 8.75 and 16.2 %). Generally, a more uniform microstructure and higher recrystallization degree can be obtained after solution treatment at the β phase region, which increases the strength and elongation of the alloy.

The precipitation of the secondary α phase can significantly improve the strength of titanium alloy [32]. Figure 9b shows the tensile properties of the alloy solution treatment at different temperatures plus aging
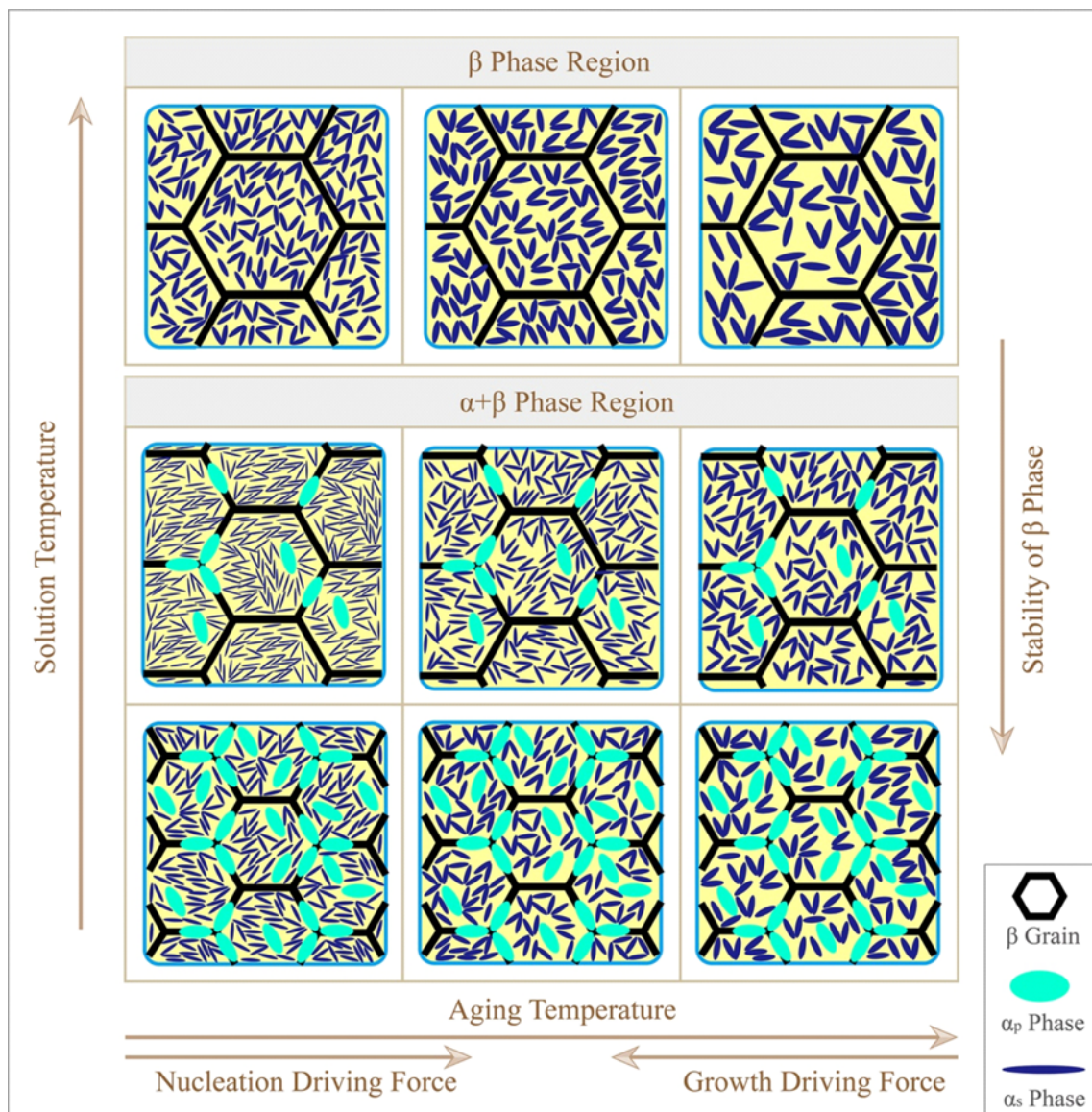
Fig. 8. Schematic illustration of the microstructure evolution after different heat treatments.

treatment at 480℃ for 4 h. Compared with the solution condition, the strength of the alloy has greatly improved. Accompanied with the solution temperature increasing from 720 to 840℃, the strength is changed from 1508 to 1630 MPa. As shown in Fig. 5, a large number of acicular secondary α phase precipitates after aging treatment. The increase of α/β phase interface can further hinder the dislocation movement, thus significantly improving the strength of the alloy [40]. There are fewer slip systems of α phase with HCP structure, which leads to the decrease of elongation (the lowest elongation at 810℃: 0.43 %). As mentioned above, the alloy has better performance in the β phase region. Different from solution treatment at α/β phase region plus aging, as shown in Fig. 9b, both the strength and elongation of the alloy increase with the increase of solution temperature after β phase

region treatment. The alloy solution treated at 720℃ plus aged at 480℃ exhibits the highest elongation (2.63 %). As shown in Fig. 8, the smaller β grain of alloy after solution treatment at a lower temperature can reduce the slip length and increase the resistance to crack nucleation, thus increasing the elongation of the alloy [39].

The aging temperature has the most apparent effect on the precipitation of the secondary α phase. Therefore, it is necessary to study the corresponding tensile properties. The variation of tensile properties data is shown in Figs. 9c,d. Notably, the strength of the alloy after solution treatment at the β phase region plus aging (UTS: from 1672 to 1344 MPa) is higher than that at the α/β phase region (UTS: from 1611 to 1218 MPa). The same result also has been obtained in the study of solution plus aging of other near-β
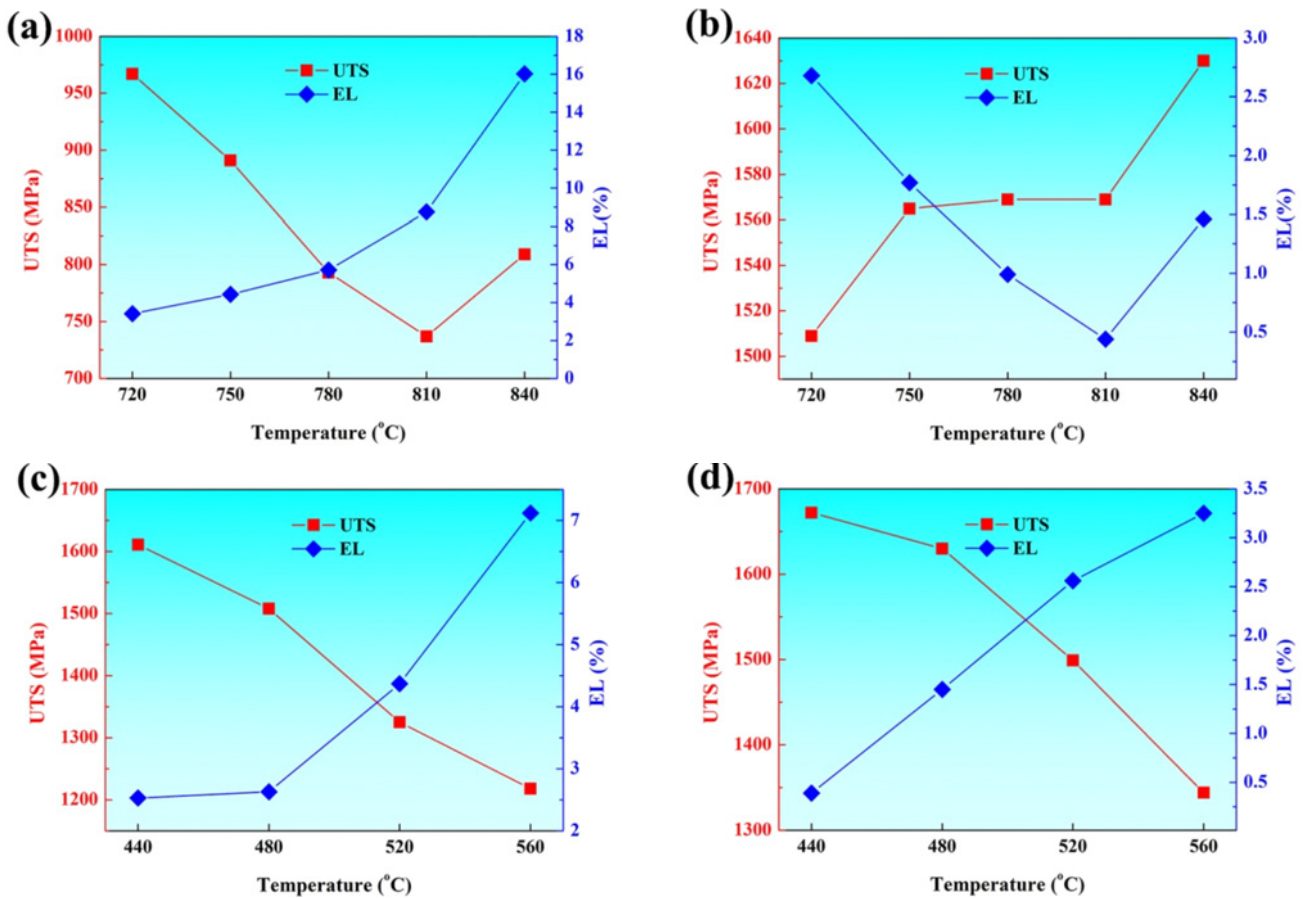
Fig. 9. Tensile properties of the alloy after (a) solution treatment at different temperatures, (b) solution treatment at different temperatures plus aging treatment at 480 ℃, solution treatment at (c) 720 ℃, and (d) 840 ℃ plus aging treatment at different temperatures.

titanium alloys [29, 33]. As shown in Figs. 6–8, compared with solution treatment at 720 ℃ plus aging, the volume fraction of secondary α phase is higher after solution treatment at 840 ℃ plus aging. This further confirms that the strength of the alloy is mainly affected by the volume fraction of the secondary α phase. Meanwhile, the incompatible deformation of the secondary α phase during the tensile testing leads to the elongation of alloy decreased. The lowest plasticity is only 0.43 % after solution treatment at 840 ℃ plus aging treatment at 440 ℃. C. L. Li et al. [41] suggested that the existence of a primary α phase can optimize the elongation of the alloy. Therefore, under the combined influence of the primary and secondary α phase, the strength and elongation of the alloy after solution treatment at 720 ℃ plus aging treatment at 440 ℃ have a better combination (UTS: 1611 MPa, EL: 2.53 %).

4. Conclusions

In summary, effects of aging and solution temperature on microstructure evolution and tensile prop-

erties of a near-β Ti-4Al-1Sn-2Zr-5Mo-8V-2.5Cr alloy were investigated systematically.

1. The volume fraction of the primary α phase and the size of β grain mainly depend on the solution treatment temperature.

2. Acicular secondary α phase precipitated after low-temperature aging treatment. The volume fraction of the secondary α phase is the largest, and the size is the smallest after solution treatment near the phase transition point plus aging treatment.

3. Secondary α phase is the most sensitive to aging treatment temperature. With the increase of aging temperature, the volume fraction of the secondary α phase decreases, and the size increases. On the other hand, after solution treatment at the β phase region plus aging, the precipitation scale of the secondary α phase increases.

4. Compared with the solution condition alloy, the strength of the aging condition alloy is significantly improved due to the precipitation of the secondary α phase. The tensile strength of the alloy after solution treatment at 840 ℃ is only 809 MPa, while it can reach 1630 MPa after aging treatment at 440 ℃.

5. With the increase of aging temperature, the ten-

sile strength increases but the plasticity decreases. After solution treatment at 720 ℃ plus aging treatment at 440 ℃, the alloy has better tensile properties: UTS: 1611 MPa, EL: 2.53 %.

Acknowledgements

References

[1] D. Eylon, R. Boyer, D. Koss, Beta Titanium Alloys in the 1990's, TMS, Denver, 1993. ISBN: 0-87339-200-0

[2] R. R. Boyer, R. D. Briggs, The use of β titanium alloys in the aerospace industry, J. Mater. Eng. Perform. 14 (2005) 681–685. doi:10.1361/105994905X75448

[3] R. R. Boyer, Attributes, characteristics, and applications of titanium and its alloys, JOM 62 (2010) 21–24. doi:10.1007/s11837-010-0071-1

[4] J. D. Cotton, R. D. Briggs, R. R. Boyer, S. Tamirisakandala, P. Russo, N. Shchetnikov, J. C. Fanning, State of the art in beta titanium alloys for airframe applications, JOM 67 (2015) 1281–1303. doi:10.1007/s11837-015-1442-4

[5] S. V. Zherebtsov, M. A. Murzinova, M. V. Klimova, G. A. Salishchev, A. A. Popov, S. L. Semiatin, Microstructure evolution during warm working of Ti-5Al-5Mo-5V-1Cr-1Fe at 600 and 800 ℃, Mat. Sci. Eng. A 563 (2013) 168–176. doi:10.1016/j.msea.2012.11.042

[6] O. M. Ivasishin, R. V. Teliovich, Potential of rapid heat treatment of titanium alloys and steels, Mat. Sci. Eng. A 263 (1999) 142–154. doi:10.1016/S0921-5093(98)01173-3

[7] A. Bhattacharjee, V. K. Varma, S. V. Kamat, A. K. Gogia, S. Bhargava, Influence of β grain size on tensile behavior and ductile fracture toughness of titanium alloy Ti-10V-2Fe-3Al, Metall. Mater. Trans. A 37 (2006) 1423–1433. doi:10.1007/s11661-006-0087-x

[8] W. Chuan, H. Liang, Hot deformation and dynamic recrystallization of a near-beta titanium alloy in the β single phase region, Vacuum 156 (2018) 384–401. doi:10.1016/j.vacuum.2018.07.056

[9] T. Furuhara, B. Poorganji, H. Abe, T. Maki, Dynamic recovery and recrystallization in titanium alloys by hot deformation, JOM 59 (2007) 64–67. doi:10.1007/s11837-007-0013-8

[10] J. H. Chen, J. S. Li, B. Tang, Y. Chen, H. C. Kou, Microstructure and texture evolution of a near β titanium alloy Ti-7333 during continuous cooling hot deformation, Prog. Nat. Sci-Mater. 29 (2019) 50–56. doi:10.1016/j.pnsc.2019.01.003

[11] T. W. Duerig, G. T. Terlinde, J. C. Williams, Phase transformations and tensile properties of Ti-10V-2Fe-3Al, Metall. Mater. Trans. A 11 (1980) 1987–1998. doi:10.1007/BF02655118

[12] Y. Y. Chen, Z. X. Du, S. L. Xiao, L. J. Xu, J. Tian, Effect of aging heat treatment on microstructure and tensile properties of a new β high strength titanium alloy, J. Alloys Compd. 586 (2014) 588–592. doi:.1016/j.jallcom.2013.10.096

[13] Z. X. Du, S. L. Xiao, L. J. Xu, J. Tian, F. T. Kong, Y. Y. Chen, Effect of heat treatment on microstructure and mechanical properties of a new β high strength titanium alloy, Mater. Design 55 (2014) 183–190. doi:10.1016/j.matdes.2013.09.070

[14] J. K. Fan, J. S. Li, H. C. Kou, K. Hua, B. Tang, Y. D. Zhang, Influence of solution treatment on microstructure and mechanical properties of a near β titanium alloy Ti-7333, Mater. Design 83 (2015) 499–507. doi:10.1016/j.matdes.2015.06.015

[15] T. T. Yao, K. Du, H. L. Wang, Z. Y. Huang, C. H. Li, L. L. Li, Y. L. Hao, R. Yang, H. Q. Ye, In situ scanning and transmission electron microscopy investigation on plastic deformation in a metastable β titanium alloy, Acta Mater. 133 (2017) 21–29. doi:10.1016/j.actamat.2017.05.018

[16] N. Yumak, K. Aslantaş, A review on heat treatment efficiency in metastable β titanium alloys: The role of treatment process and parameters, J. Mater. Sci. Tech. 9 (2020) 15360–15380. doi:10.1016/j.jmrt.2020.10.088

[17] D. Banerjee, J. C. Williams, Perspectives on titanium science and technology, Acta Mater. 61 (2013) 844–879. doi:10.1016/j.actamat.2012.10.043

[18] S. A. Mantri, D. Choudhuri, T. Alam, G. B. Viswanathan, J. M. Sosa, H. L. Fraser, R. Banerjee, Tuning the scale of α precipitates in β-titanium alloys for achieving high strength, Scr. Mater. 154 (2018) 139–144. doi:10.1016/j.scriptamat.2018.05.040

[19] W. G. Zhu, Q. Y. Sun, C. S. Tan, P. Li, L. Xiao, J. Sun, Tensile brittleness and elongation improvement in a novel metastable β titanium alloy with lamella structure, J. Alloys Compd. 827 (2020) 154311. doi:10.1016/j.jallcom.2020.154311

[20] B. He, J. Li, X. Cheng, H. M. Wang, Brittle fracture behavior of a laser additive manufactured near-β titanium alloy after low temperature aging, Mat. Sci. Eng. A 699 (2017) 229–238. doi:10.1016/j.msea.2017.05.050

[21] D. Y. Qin, Y. L. Li, S. Y. Zhang, L. Zhou, On the tensile embrittlement of lamellar Ti-5Al-5V-5Mo-3Cr alloy, J. Alloys Compd. 663 (2016) 581–593. doi:10.1016/j.jallcom.2015.12.158

[22] J. Wu, Z. D. Lv, C. J. Zhang, J. C. Han, H. Z. Zhang, S. Z. Zhang, H. Muhammad, P. Cao, Investigation of the deformation mechanism of a near β titanium alloy through isothermal compression, Metals 7 (2017) 498. doi:10.3390/met7110498

[23] Z. D. Lü, C. J. Zhang, Z. X. Du, J. C. Han, S. Z. Zhang, F. Yang, Y. Y. Chen, Relationship between microstructure and tensile properties on a near-β titanium alloy after multidirectional forging and heat treatment, Rare Metals 38 (2019) 336–342. doi:110.1007/s12598-018-1159-y

[24] C. Leyens, M. Peters, Titanium and Titanium Alloys: Fundamentals and Applications, Wiley-VCH, Weinheim, 2003. ISBN: 978-3-527-60211-7

[25] N. G. Jones, R. J. Dashwood, D. Dye, M. Jackson, Thermomechanical processing of Ti-5Al-5Mo-5V-3Cr, Mat. Sci. Eng. A 490 (2008) 369–377. doi:10.1016/j.msea.2008.01.055

[26] J. W. Lu, P. Ge, Y. Q. Zhao, Recent development of effect mechanism of alloying elements in titanium alloy design, Rare Metal. Mat. Eng. 43 (2014) 775–779. doi:10.1016/S1875-5372(14)60082-5

[27] J. W. Xu, W. D. Zeng, H. Y. Ma, D. D. Zhou, Static globularization mechanism of Ti-17 alloy during heat treatment, J. Alloys Compd. 736 (2018) 99–107. doi:10.1016/j.jallcom.2017.11.117

[28] I. Weiss, S. L. Semiatin, Thermomechanical processing of beta titanium alloys—An overview, Mat. Sci. Eng. A 243 (1998) 46–65. doi:10.1016/S0921-5093(97)00783-1

[29] S. Shekhar, R. Sarkar, S. K. Kar, A. Bhattacharjee, Effect of solution treatment and aging on microstructure and tensile properties of high strength β titanium alloy, Ti-5Al-5V-5Mo-3Cr, Mater. Design 66 (2015) 596–610. doi:10.1016/j.matdes.2014.04.015

[30] T. Furuhara, T. Maki, Variant selection in heterogeneous nucleation on defects in diffusional phase transformation and precipitation, Mat. Sci. Eng. A 312 (2001) 145–154. doi:10.1016/S0921-5093(00)01904-3

[31] L. Ren, W. L. Xiao, H. Chang, Y. Q. Zhao, C. L. Ma, L. Zhou, Microstructural tailoring and mechanical properties of a multi-alloyed near β titanium alloy Ti-5321 with various heat treatment, Mat. Sci. Eng. A 711 (2018) 553–561. doi:10.1016/j.msea.2017.11.029

[32] J. W. Lu, Y. Q. Zhao, P. Ge, Y. S. Zhang, H. Z. Niu, W. Zhang, P. X. Zhang, Precipitation behavior and tensile properties of new high strength beta titanium alloy Ti-1300, J. Alloys Compd. 637 (2015) 1–4. doi:10.1016/j.jallcom.2015.02.222

[33] S. Sadeghpour, S. M. Abbasi, M. Morakabati, S. Bruschi, Correlation between alpha phase morphology and tensile properties of a new beta titanium alloy, Mater. Design 121 (2017) 24–35. doi:10.1016/j.matdes.2017.02.043

[34] Z. X. Du, S. L. Xiao, Y. P. Shen, J. S. Liu, J. Liu, L. J. Xu, F. T. Kong, Y. Y. Chen, Effect of hot rolling and heat treatment on microstructure and tensile properties of high strength beta titanium alloy sheets, Mat. Sci. Eng. A 631 (2015) 67–74. doi:10.1016/j.msea.2015.02.030

[35] S. Nag, Y. Zheng, R. E. A. Williams, A. Devaraj, A. Boyne, Y. Wang, P. C. Collins, G. B. Viswanathan, J .S. Tiley, B. C. Muddle, R. Banerjee, H. L. Fraser, Non-classical homogeneous precipitation mediated by compositional fluctuations in titanium alloys, Acta Mater. 60 (2012) 6247–6256. doi:10.1016/j.actamat.2012.07.033

[36] Y. Zhou, K. Wang, R. L. Xin, Q. Liu, Effect of special primary α grain on variant selection of secondary α phase in a near-α titanium alloy, Mater. Lett. 271 (2020) 127766. doi:10.1016/j.matlet.2020.127766

[37] D. Wu, L. B. Liu, L. J. Zeng, W. G. Zhu, W. L. Wang, X. Y. Zhang, J. F. Hou, B. L. Liu, J. F. Lei, K. C. Zhou, Designing high-strength titanium alloy using pseudo-spinodal mechanism through diffusion multiple experiment and CALPHAD calculation, J Mater. Sci. Tech. 74 (2021) 78–88. doi:10.1016/j.jmst.2020.10.013

[38] X. Zhang, H. C. Kou, J. S. Li, F. S. Zhang, L. Zhou, Evolution of the secondary α phase morphologies during isothermal heat treatment in Ti-7333 alloy, J. Alloys Compd. 577 (2013) 516–522. doi:10.1016/j.jallcom.2013.06.180

[39] G. Lütjering, J. Albrecht, C. Sauer, T. Krull, The influence of soft, precipitate-free zones at grain boundaries in Ti and Al alloys on their fatigue and fracture behavior, Mat. Sci. Eng. A 468–470 (2007) 201–209. doi:10.1016/j.msea.2006.07.168

[40] P. Castany, M. Besse, T. Gloriant, In situ TEM study of dislocation slip in a metastable β titanium alloy, Scr. Mater. 66 (2012) 371–373. doi:10.1016/j.scriptamat.2011.11.036

[41] C. L. Li, X. J. Mi, W. J. Ye, S. X. Hui, Y. Yu, W. Q. Wang, Effect of solution temperature on microstructures and tensile properties of high strength Ti-6Cr-5Mo-5V-4Al alloy, Mat. Sci. Eng. A 578 (2013) 103–109. doi:10.1016/j.msea.2013.04.063